

Uranium Adsorption Using a Composite Material Based on Platelet SBA-15 Supported Tin Salt Tungstomolybdophosphoric Acid

H. Aghayan, F. A. Hashemi, R. Yavari, S. Zolghadri

Abstract—In this work, a new composite adsorbent based on a mesoporous silica SBA-15 with platelet morphology and tin salt of tungstomolybdophosphoric (TWMP) acid was synthesized and applied for uranium adsorption from aqueous solution. The sample was characterized by X-ray diffraction, Fourier transfer infra-red, and N_2 adsorption-desorption analysis, and then, effect of various parameters such as concentration of metal ions and contact time on adsorption behavior was examined. The experimental result showed that the adsorption process was explained by the Langmuir isotherm model very well, and predominant reaction mechanism is physisorption. Kinetic data of adsorption suggest that the adsorption process can be described by the pseudo second-order reaction rate model.

Keywords—Platelet SBA-15, tungstomolybdophosphoric acid, adsorption, uranium ion.

I. INTRODUCTION

URANIUM contamination in the environment as a result of the development of nuclear technology and application of that in its related industries is a serious problem for living being and damage of bioorganic due to its high chemical and radiological toxicity [1]. Therefore, the efficient removal and recovery of uranium from waste has been of researcher's interest. Many methods such as chemical precipitation [2], solvent extraction [3], biosorption [4], adsorption, ion exchange [5], and membrane processes [6] have been developed for the removal of uranium from waste water. Among them, adsorption has proved to be an attractive method because of its high selectivity, rapid uptake, low cost, easy-to-handling, and their availability [7].

Mesoporous silica materials such as MCM-41, MCM-48, FSM-16, and MSU-1 have been applied successfully in the field of some metal ions separation [8].

SBA-15, as a member of this family having large BET surface area, large pore, diameter, and high hydrothermal stability [9], has proved to be very promising candidate for adsorption of metal ions [10]. In this regard, the different morphologies of SBA-15 such as fine powders, fibers, membranes and spheres have been prepared [11]. However, platelet morphology due to its short channel lengths and

greater pore accessibility which leads to the lowest steric diffusion resistance and fastest transport of the ions from the solution to the pores has been of great interest to enable for practical application [11]. Nevertheless, mesoporous silica suffers from lack of the appropriate surface properties for many applications. One of the ways to improve the surface property and increase the adsorption capacity of SBA-15 is to immobilize of materials having high potential toward metal ions adsorption on the support. Heteropoly acids known as polyoxometalate due to high strong exchangeable acidic protons in their structures have such capability [12]. Since 1970 decade, the efforts for the preparation of new material based on polyoxometalates with the special properties for the removal of toxic and hazardous radioisotopes from nuclear wastewater have been increased. However, the limited studies have been performed on the synthesis and adsorption characteristic of polyoxometalates/mesoporous silica composite materials, which have high affinity toward uranium ions. Therefore, the aim of the present study was to prepare the new composite material based on Tin salt of tungstomolybdophosphoric (TWMP) acid and platelet morphology of SBA-15 to investigate the adsorption behavior of uranium ions on this material under various operation conditions.

II. MATERIALS AND METHODS

A. Chemicals

All chemicals used in these experiments, P123 (poly (ethylene oxide)-poly (propylene oxide)-poly (ethylene oxide) (EO20-PO70-EO20), tetraethyl orthosilicate (TEOS 98%), absolute ethanol (99.98%), fuming hydrochloric acid (HCl 37%), titanium chloride ($TiCl_4$), Zirconium chloride ($ZrOCl_2 \cdot 8H_2O$) sodium molybdate. Sodium tungstate, sodium hydrogen sulphate and concentrated sulfuric acid (H_2SO_4 85%) were prepared from analytical reagent grade chemicals and obtained from E. Merck or Fluka companies. A stock solution of uranium (1000 mg L⁻¹) was prepared by dissolving the definite amount of uranyl nitrate in nitric acid solution of 0.3 M. The solution was further diluted with demineralized water.

B. Preparation of Samples

Platelet mesoporous silica SBA-15 was prepared according to the literature method described elsewhere [13]. In a typical synthesis, 2.0 g of P123 and 0.5 g of $ZrOCl_2 \cdot 8H_2O$ was mixed in 60 cm³ of 2 M HCl and 15 cm³ of demineralized water

F. A. Hashemi is with Material and Nuclear Fuel Research School, Nuclear Science and Technology Research Institute (NSTRI), P.O. Box. 11365-8486, Tehran, Iran (corresponding author, e-mail: fhashemi@aeoi.org.ir).

H. Aghayan, R. Yavari and S. Zolghadri are with Material and Nuclear Fuel Research School, Nuclear Science and Technology Research Institute (NSTRI), P.O. Box. 11365-8486, Tehran, Iran.

(DMW). The solution was stirred for 30 minutes until the surfactant was dissolved completely. Then, 4.4 g of tetraethyl orthosilicate (TEOS) was added dropwise to this solution at 40 °C, stirred for 24h and transferred to an autoclave for hydrothermal treatment at 100 °C for 24h. Finally, the resulting precipitate was filtered, washed carefully with distilled water, and air dried. Surfactant was removed by calcination at 550 °C for 6h in air.

$H_3[PMo_6W_6O_{40}] \cdot nH_2O$ was prepared according to the procedure of Huixiong et al. denoted as HMWP [14]. Tin salt of HMWP was supported on mesoporous silica SBA-15 as the follow procedure: 0.3 gr of $SnCl_4 \cdot 5H_2O$ was dissolved in aqueous containing 0.3 M HCl and then 1 g of SBA-15 was added to above solution, stirred at 100 °C until the solvent volatilized. Subsequently, the precipitate was collected and dispersed in 10 ml of aqueous solution of heteropolyacid. The sample was filtered, washed with deionized water and ethanol, and dried at 40 °C overnight. The obtained product was then immersed in acid (HNO_3 , 0.1M) to be converted to the H^+ form.

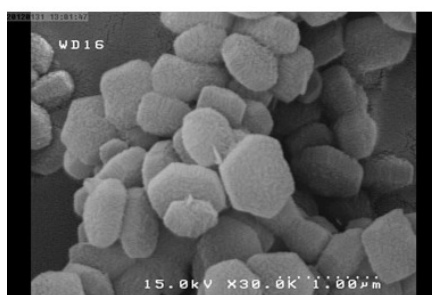
C. Adsorption Studies

The adsorption capacities and percentage of uranium ions were determined by batch technique. For this purpose, 0.05 g of dried solid samples was kept in a 20 ml of desired concentration of uranium ion solution while this mixture was continuously shaken in water bath at 150 rpm and then centrifuged at 4000 rpm for 5 min. Then, the concentration of uranium in aqueous solution before and after experiment was measured by ICP-OES elemental analysis. The adsorption percentage of uranium (P) and its capacity (q_e) was calculated by the following equations (1) and (2), respectively.

$$P = (1 - C_e/C_0) \times 100\% \quad (1)$$

$$q_e = ((C_0 - C_e)v)/M \quad (2)$$

where C_0 and C_e are the uranium concentration in initial and



equilibrium solution ($mg \cdot L^{-1}$), v is the volume of the solution in L, and M is the mass of the adsorbent in gram.

D. Characterization of Sample

Fig. 1 shows small angle XRD patterns of the pure synthesized SBA-15 mesoporous silica and TWMP immobilized on SBA-15 support respectively. It is clear from Fig. 1 that both of them show similar three well-resolved peaks in the 2θ range of 0.8 to 3, which can be indexed to the (100), (110), and (200) diffraction peaks of a two-dimensional hexagonal symmetry ($p6mm$) pattern. These peaks are detectable as a weaker intensity peaks with a slight shift from low angles to the higher angles in the XRD patterns of the SBA-15-TWMP. This phenomenon, indicating the decrease in d-spacing as a result of the occupying mesoscopic channels of silica by TWMP, reveals the preservation of the hexagonal pore structure [15].

Fig. 2 shows the SEM images of the sample. It is observed that the prepared sample presents platelet morphologies. Platelet morphology is a combination of uniform tablets, and most of them have regular hexagonal tablets consisting of eight crystal faces, two hexagonal and six rectangular symmetries. The diameter and thickness of tablets are approximately 1-2 μm and 200-250 nm, respectively.

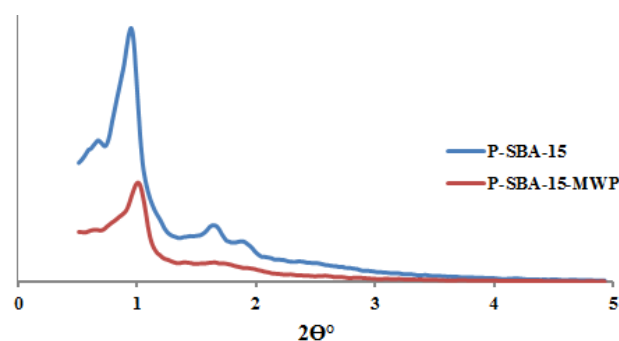


Fig. 1 Small angle XRD patterns of SBA-15 and SBA-15-TWMP

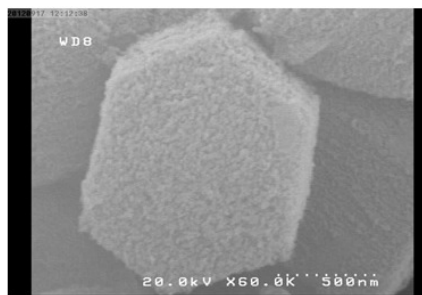


Fig. 2 SEM image of mesoporous silica SBA-15 with platelet morphology

The FT- IR spectra of pristine SBA-15, SBA-15-TWMP, and HMWP have been shown in Fig. 3. The bands observed in the spectrum of pure SBA-15 at 1037 and 806 cm^{-1} belong to the stretching vibrations of Si-O-Si and Si-O. Also, the peaks at 840 cm^{-1} , 948 cm^{-1} , and 1072 cm^{-1} which are seen in the spectrum of HMWP are characterization of symmetric stretching of the M-O-M, M=O or W=O bond and P-O bond

[16]. The presence of broad band observed in the FT-IR spectrum of the composite material in the reign of 900-1200 cm^{-1} is due to the overlap of P-O and W=O or M=O bands in HMWP material with those of Si-O-Si stretching vibration of mesoporous supporter. These obtained results confirm that TWMP have been immobilized successfully onto the SBA-15 mesoporous supporter.

Fig. 4 shows the N₂ adsorption-desorption isotherms and the corresponding BJH pore size distribution curve of SBA-15 and SBA-15-TWMP respectively and the detail physical properties are summarized in Table I. As can be seen in the curve of SBA-15, there is a sharp inflection capillary condensation step at relative pressure between 0.6-0.9 suggesting the presence of uniform mesoporous. All of mentioned physical properties are decrease after immobilization of TWMP onto the pore of SBA-15. This can be explained by the fact that the occupation of the pore of SBA-15 with TWMP has been performed successfully.

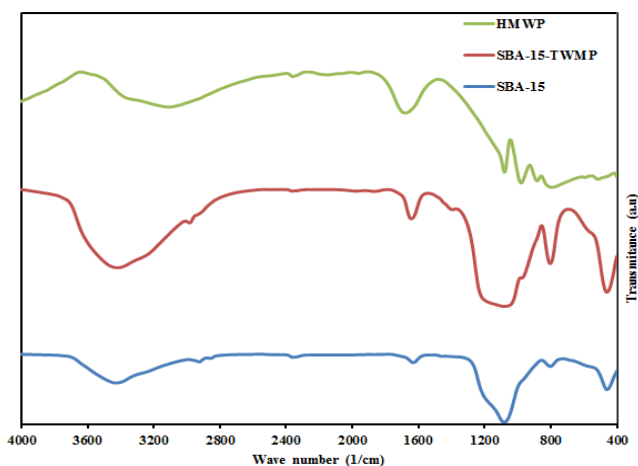


Fig. 3 The IR spectra of pure mesoporous silica, SBA-15-TWMP and HMWP

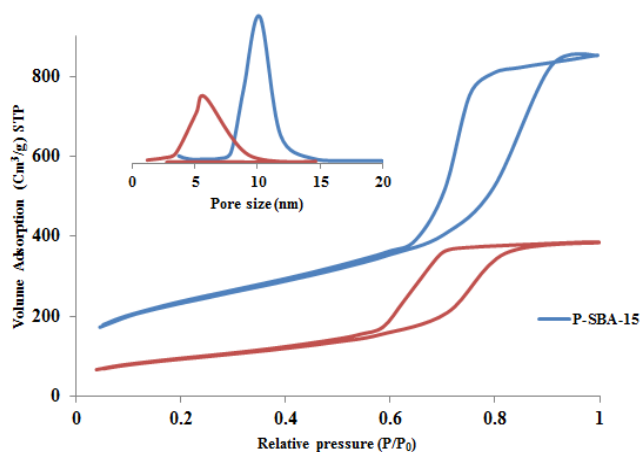


Fig. 4 N₂ adsorption- desorption isotherms of pure SBA-15 and SBA-15- MWP

TABLE I
BET SURFACE AREAS, PORE SIZE AND PORE VOLUME OF SBA-15 AND P-SBA-15-MWP

No. S		BET surface area (m ² /g)	Por size (nm)	Por volume (cm ³ /g)
5	P-SBA-15	724	10.2	1.2
6	P-SBA-15-MWP	367	5.8	0.71

E. Adsorption Studies

1. Adsorption Isotherms

To provide key information for designing a favorable adsorption system, experiments were accomplished in the range 20-1000 ppm of concentration. As shown in Fig. 5, the amount of uranium adsorbed on the composite increases with a rise in initial concentration of uranium ion and the maximum adsorption of uranium reaches 117 mg.g⁻¹ at equilibrium UO₂²⁺ concentration of 700 mg.l⁻¹. The obtained equilibrium data from these experiments can be analyzed by various types of statistical isotherm models which are ordinarily applied to describe the manner of distribution of the solutes between liquid and solid phase at various equilibrium concentration. Among the various types of mathematical models, Langmuir, Freundlich and Dubinin-Radushkevich (D-R) equations are mostly used for aqueous solution treatment applications. In general, these models are characterized by certain constant values which describe the surface properties of the sorbents and their affinities toward cations and anions, and therefore, they can use to assess their adsorption capacities. In order to obtain the constants of these isotherm models, the linear plots of these equations were depicted in Fig. 5 (b) (Langmuir model), Fig. 5 (c) (Freundlich model) and Fig. 5 (d) (Dubinin-Radushkevich model). Consequently, from the slope and intercept of these linear plots, these constants were calculated and tabulated in Table II. These models assume that

1. Langmuir: Surface is homogeneous and each active site can accommodate only one ion.
2. Freundlich: The adsorbent has heterogeneous surface thus it can be applied to multilayer adsorption
3. Dubinin-Radushkevich: This model is commonly used to express the adsorption mechanism with a Gaussian energy distribution onto both homogeneous and heterogeneous surfaces [17].

The linear expression of these isotherm models can be represented by the following equation:

1. Langmuir:

$$\frac{C_e}{q_e} = \frac{1}{ba} + \frac{C_e}{a} \quad (3)$$

where q_e is the equilibrium amount of uranium ion adsorbed per gram C_e is the equilibrium concentration of uranium ion in solution (mg.dm⁻³), b is the Langmuir constant related to the affinity of binding active sites (dm³.mg⁻¹), and a is the maximum sorption capacity of adsorbent (mg.g⁻¹).

2. Freundlich

$$\log q_e = \log k_f + \frac{1}{n} \log c_e \quad (4)$$

where K_f (L.g⁻¹) and n are the Freundlich constants describing the adsorption capacity and adsorption intensity, respectively.

3. Dubinin-Radushkevich:

$$\ln q_e = \ln q_{DR} - B_{DR} \epsilon^2 \quad (5)$$

where q_{DR} (mmol.g⁻¹) and B_{DR} (mol².J⁻²) are the Dubinin-

Radushkevich constants representing the theoretical saturation capacity and the mean free energy of adsorption per mole of the adsorbate, respectively. Also, ε is the apparent free energy ($\text{kJ}\cdot\text{mol}^{-1}$) which is expressed by;

$$\varepsilon = RT \ln \left(1 + \frac{1}{C_e} \right) \quad (6)$$

where R is the ideal gas constant ($8.314 \text{ J}\cdot\text{mol}^{-1}\cdot\text{K}^{-1}$), and T is the absolute temperature of adsorption (K). By using the linear plot of $\text{Ln}qe$ versus ε^2 and obtaining the constant of B_{DR} from the slop of this linear plot, one of the important parameters of Dubinin-Radushkevich equation (E ($\text{kJ}\cdot\text{mol}^{-1}$)) which estimates the type of sorption process is calculated by;

$$E = \frac{1}{\sqrt{2B_{DR}}} \quad (7)$$

If $1 < E < 8$, a dominant mechanism is the physical sorption while if the amount of E to be placed in the range of 8-16, the chemical sorption becomes a dominant mechanism [18]. As

can be seen from this table, in the range of the studied concentration, the values of the correlation coefficients of the linear regressions (R^2) as a criterion for the evaluation of the adsorption data with isotherm adsorption models show that this value for Langmuir model was found to be higher ($R^2=0.9917$) than the others. It indicates that this model has good agreement with the experimental data. This phenomenon is due to the homogeneous and uniform distribution of sorption active site on the surface of SBA-15-TWMP. Also, based on the result depicted in Table II, the obtained amount for R_L (0.1) shows that the adsorption process is favorable. On the other hand, the amount of R^2 for Dubinin-Radushkevich indicates that this isotherm gives good explanation about the adsorption process. As can be seen from this table, the obtained E value ($3.99 \text{ kJ}\cdot\text{mol}^{-1}$) is smaller than 8 and higher than 1, which shows that the predominant reaction mechanism is physisorption process. At the same time, the positive value of E indicates the endothermic nature of the process.

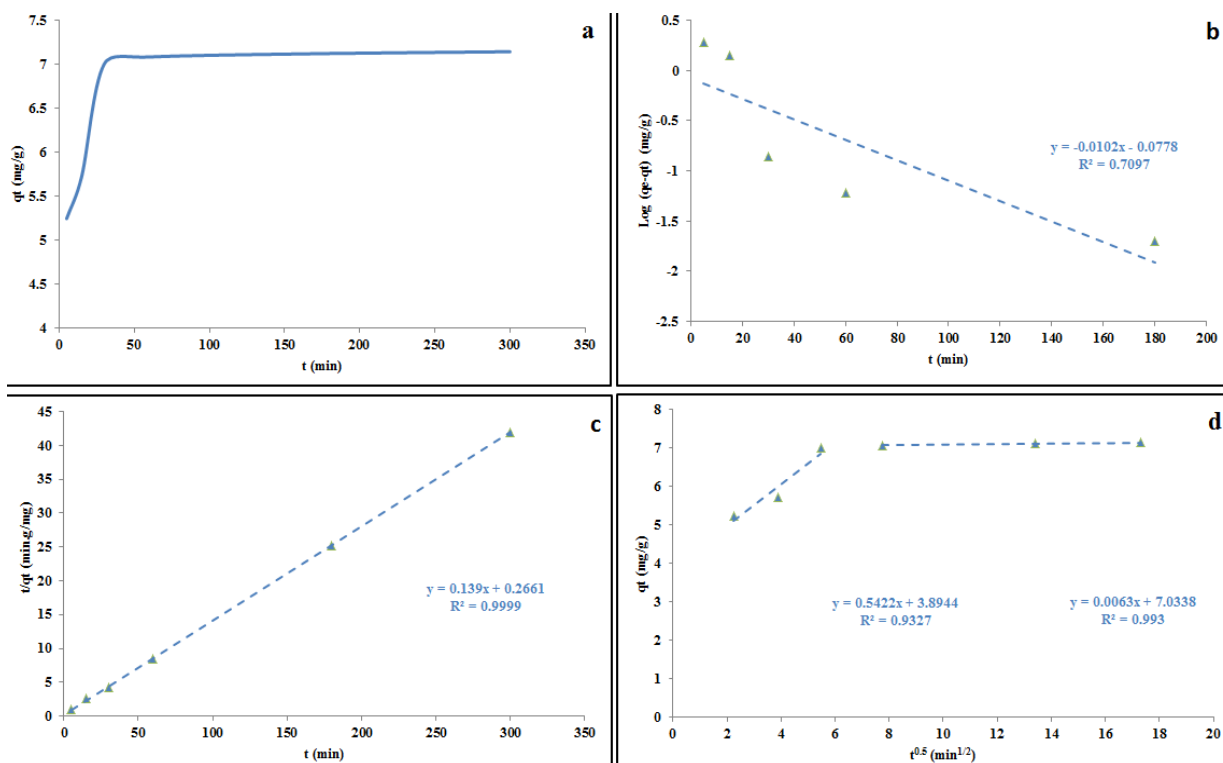


Fig. 5 Adsorption isotherm (a). Langmuir (b), Freundlich (c) and Dubinin-Radushkevich (d) linear plot, of uranium ion onto SBA-15-TWMP. pH=5, t = 24 h, T = 25 °C, agitation rate = 180 rpm

TABLE II
LANGMUIR, FRUNDLICH, AND DUBININ-RADUSHKEVICH PARAMETERS FOR ADSORPTION OF URANIUM BY SBA-15-TWMP

U	Langmuir			Freundlich			Dubinin-Radushkevich	
	a(mg/g)	b (l/mg)	R ²	K _f	n	R ²	E (kj mol ⁻¹)	R ²
	117.64	0.01	0.996	5.34	1.96	0.883	4.3	0.9716

2. Adsorption Kinetics

The kinetic study was examined by suspending heteropoly acid supported sample into a stirred metal ion solution at

various contact time, while the other parameters such as concentration of metal ions (20ppm), temperature (room temperature) and pH (3.5) were kept constant. As can be seen

from Fig. 6, the adsorption of uranium onto SBA-15-TWMP was increased rapidly in the initial 30 minutes of contact time and then reaches more slowly to the equilibrium time.

The obtained results from contact time experiment were used to simulate the kinetic adsorption data and to further explain the controlling mechanism of adsorption processes like mass transfer and chemical reaction process of uranium onto SBA-15-TWMP. In this regard, in the present work, three models of kinetic reaction including pseudo-first-order, pseudo-second-order and Intraparticle diffusion model were used to simulate the kinetic adsorption data of uranium on SBA-15-TWMP. The linearized forms of these semi-empirical kinetic model equations are given as, respectively;

$$\log(q_e - q_t) = \log q_e - \frac{k_1}{2.303} t \quad (8)$$

$$\frac{t}{q_t} = \frac{1}{k_2 q_e^2} + \frac{1}{q_e} t \quad (9)$$

$$q_t = k_d t^{1/2} + c \quad (10)$$

where q_e and q_t are the adsorbed amounts of metal at equilibrium and at time t expressed as mg.g^{-1} ; k_1 , k_2 and k_d are the pseudo-first-order, pseudo-second-order and diffusion rate constant expressed as min^{-1} , $\text{g.mg}^{-1}.\text{min}^{-1}$ and $\text{mg.g}^{-1}.\text{min}^{-1}$ respectively, and c is the intercept at the ordinate in mg.g^{-1} . Figs. 6 (b)-(d) show linear plots of these equations. Linear arrangements are commonly used to check the validity of these models and to obtain the model parameters when the corresponding linear plot is adequate. As shown, among these kinetic models, the higher correlation coefficient ($R^2 > 0.997$) corresponded to the pseudo-second-order model shows that this model fitted well the kinetic data.

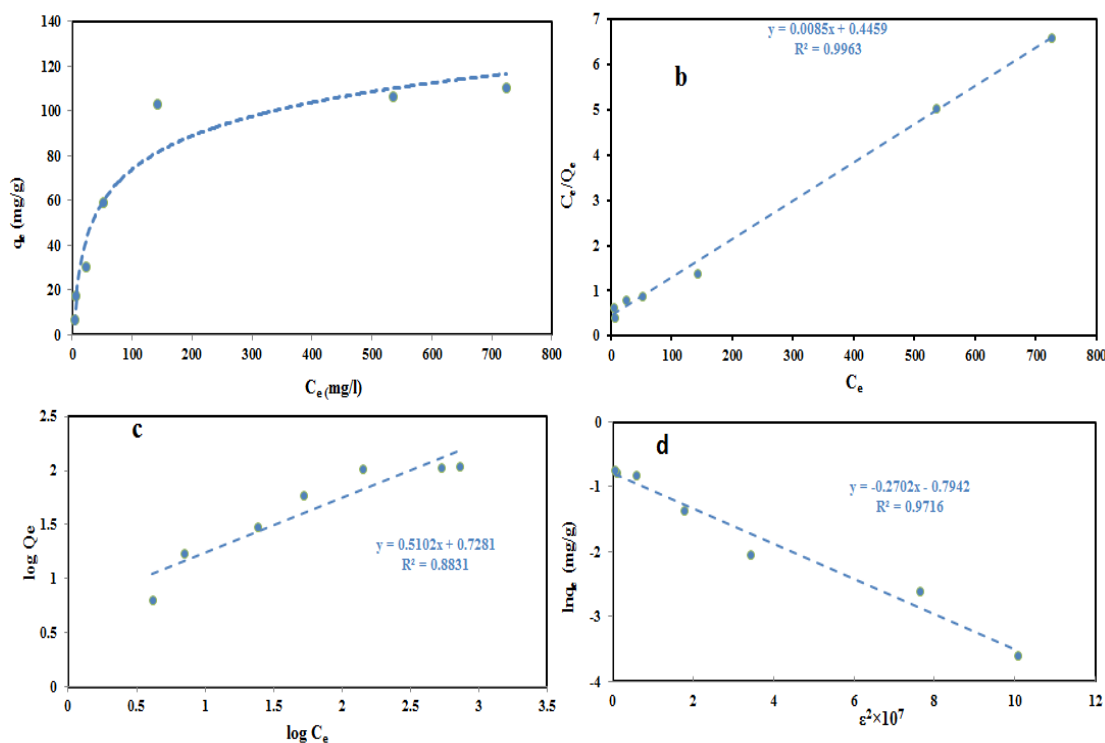


Fig. 6 Rate of adsorption (a) and pseudo-first-order (b), pseudo-second-order (c) and Weber- Morris models (d)

III. CONCLUSION

In the present research work, we benefit from the abilities of platelet structure of SBA-15 as a support for an adsorbent and stannic TWMP as the adsorbent in the single material named composite SBA-15-TWMP. The immobilization of TWMP on SBA-15 confirms by FT-IR, XRD, and BET analysis. The adsorption behavior of uranium onto hybrid shows that maximum adsorption of uranium reaches 117 mg.g^{-1} at $\text{pH}=3.5$ and 60 minutes of contact time. The homogeneous distribution of sorption active site on the surface of SBA-15-TWMP indicates that Langmuir isotherm model has good agreement with the experimental data. The obtained E value (by using Dubinin-Radushkevich model) infers that the

predominant reaction mechanism is physicosorption process and the adsorption process has endothermic nature. The obtained results show that the kinetics behavior of uranium adsorption on SBA-15-TWMP matches very well with a pseudo-second-order rate equation, and intra-particle diffusion of uranium ion is the rate controlling stage. Overall, based on the obtained results ($q_{\text{max}}=117 \text{ mg.g}^{-1}$ at $\text{pH}=6$ and $\text{time}=30$ hour), it shows that this new composite material can be a very good candidate for the removal of uranium ion from aqueous solution.

ACKNOWLEDGMENT

The authors wish to thank Nuclear Sciences and

Technology Research Institute (NSTRI) for financial supports

REFERENCES

- [1] Zhang, Z. B., Yu, X. F., Cao, X. H., Hua, R., Li, M., Liu, Y. H. 2014. Adsorption of U(VI) from aqueous solution by sulfonated ordered mesoporous carbon. *J. Radioanal. Nucl. Chem.* 301,821–830.
- [2] Djedidi, Z., Bouda, M., Souissi, M. A., Cheikh, R. B., Mercier, G., Tyagi, R. D., Blais, J.F. 2009 Metals removal from soil, fly ash and sewage sludge leachates by precipitation and dewatering properties of the generated sludge. *J. Hazard. Mater.* 172,1372–1382.
- [3] Kumari, N., Prabhu, D., Pathak, P., Kanekar, A., Manchanda, V., 2011. Extraction studies of uranium into a third-phase of thorium nitrate employing tributyl phosphate and N,N-dihexyl octanamide as extractants in different diluents. *J. Radioanal. Nucl. Chem.*, 289,835–843.
- [4] Ghasemi, M., Keshtkar, A. R., Dabbagh, R., Safdari, S. J., 2011. Biosorption of uranium (VI) from aqueous solutions by Ca-pretreated *Cystoseira indica* alga: breakthrough curves studies and modeling. *J. Hazard. Mater.* 189,141–149.
- [5] Fan, Q., Li, P., Chen, Y., Wu, W.S., 2011, Preparation and application of attapulgite/iron oxide magnetic composites for the removal of U (VI) from aqueous solution. *J. Hazard. Mater.* 192,1851–185.
- [6] Shen, J., Schafer, A., 2014. Removal of fluoride and uranium by nanofiltration and reverse osmosis: A review. *Chemosphere.* 117,679–691.
- [7] Asadollahi, N., Yavari, R., Ghanadzadeh, H., 2015. Preparation, characterization and analytical application of stannic molybdophosphate immobilized on multiwalled carbon nanotubes as a new adsorbent for the removal of strontium from wastewater. *J. Radioanal. Nucl. Chem.* 303,2445–2455.
- [8] Singer, D. M., Guo, H., Davis, J. A., 2014. U(VI) and Sr(II) batch sorption and diffusion kinetics into mesoporous silica (MCM-41). *Chem. Geol.* 390,152–163.
- [9] Amit Katiyar, A., Santosh Yadav, S., Smirmiotis, P.G., Pinto, N.G., 2006. Synthesis of ordered large pore SBA-15 spherical particles for adsorption of biomolecules. *J. Chromatogr. A.* 1122,13–20.
- [10] Ahmadi, M., Yavari, R., Faal, A. Y., Aghayan, H., 2016. Preparation and characterization of titanium tungstophosphate immobilized on mesoporous silica SBA-15 as a new inorganic composite ion exchanger for the removal of lanthanum from aqueous solution. *J. Radioanal. Nucl. Chem.* 310,177–190.
- [11] Zhu, W., Li, X., Wu, D., Yu, J., Zhou, Y., Luo, Y., Wei, K., Ma, W., 2016. Synthesis of spherical mesoporous silica materials by pseudomorphic transformation of silica fume and its Pb²⁺ removal properties. *Micropor. Mesopor. Mat.* 222,192–201.
- [12] Yavari, R., Ahmadi, S.J., Huang, Y.D., Khanchi, A.R., Bagheri, G., He, J.M., 2009. Synthesis, characterization and analytical application of a new inorganic cation exchanger—Titanium(IV) molybdophosphate. *Talanta.* 77,1179–1184.
- [13] C. Shih-Yuan, T. Chih-Yuan, C. Wei-Tsung, L. Jey-Jau, A Facile Route to Synthesizing Functionalized Mesoporous SBA-15 Materials with Platelet Morphology and Short Mesochannels, *Chem. Mater.* 20 (2008) 3906.
- [14] Huixiong, W., Mei, Z., Yixin, Q., Haixia, L., Hengbo, Y., 2009. Preparation and Characterization of Tungsten-substituted Molybdophosphoric Acids and Catalytic Cyclodehydration of 1,4-Butanediol to Tetrahydrofuran. *Chin. J. Chem. Eng.* 17,200–206.
- [15] Aghayan, H., Mahjoub, A. R., Khanchi, A. R., 2013. Samarium and dysprosium removal using 11-molybdo-vanadophosphoric acid supported on Zr modified mesoporous silica. *Chem. Eng. J.* 225,509–519.
- [16] Karimi, Z., Mahjoub, A. R., Davari Aghdam, F., 2009. SBA immobilized phosphomolybdic acid: Efficient hybrid mesostructured heterogeneous catalysts. *J. Colloid. Interface. Sci.* 337,420–426.
- [17] Chen, X., 2015. Modeling of Experimental Adsorption Isotherm Data. *Information.* 6,14–22.
- [18] Dada, A. O., Olalekan, A. P., Olatunya, A. M. 2012. Langmuir, Freundlich, Temkin and Dubinin–Radushkevich Isotherms Studies of Equilibrium Sorption of Zn²⁺ onto Phosphoric Acid Modified Rice Husk. *J. Appl. Chem.* 3,38–45.